J Appl Biomed
DOI: 10.32725/jab.2021.011
journal homepage: http://jab.zsf.jcu.cz

Journal of Applied Biomedicine

Original research article

Echinacoside alleviates acetaminophen-induced liver injury by attenuating oxidative stress and inflammatory cytokines in mice

Mya Thida [1, 4], Ben Li [1], Xiaoyao Zhang [1], Chen Chen [1] *, Xiaoying Zhang [1, 2, 3] *

[1] *Shaanxi University of Technology, College of Biological Science and Engineering, Chinese-German Joint Laboratory for Natural Product Research, Hanzhong, Shaanxi, China*
[2] *University of Minho, Department of Biology, Centre of Molecular and Environmental Biology, Campus de Gualtar, Braga, Portugal*
[3] *Northwest A&F University, College of Veterinary Medicine, Yangling, China*
[4] *Ministry of Education, Biotechnology Research Department, Kyaukse, Myanmar*

Abstract
This study evaluates the protective effect of Echinacoside on acute liver toxicity induced by acetaminophen in mice and the mechanism behind it. Echinacoside and N-Acetyl Cysteine were intragastrically administrated for 7 days, and acetaminophen was intraperitoneally injected into mice 1 h after the last treatment on day 7. At the end of the experimental period, histological examination, parameters for the level of oxidative damage, hepatic malondialdehyde, serum pro-inflammatory cytokines (tumor necrosis factor-α, interleukin-6, and interleukin-1β), UDP-glucuronosyltransferases, and sulfotransferases changes were examined using enzyme-linked immunosorbent assay and standard biochemical procedures. The expression of cytochrome P450 2E1 protein was assessed by western blot, followed by *in silico* molecular docking. Acetaminophen treatment obviously increased the levels of ALT and AST, changed hepatic histopathology, promoted oxidative stress, decreased antioxidant enzyme activities, and elevated the pro-inflammatory cytokines. Echinacoside significantly attenuated Acetaminophen-induced liver damage in a dose-dependent manner, with the most effective dose at 100 mg/kg. The pretreatments of Echinacoside in different concentrations altered the Acetaminophen-induced hepatotoxicity levels by decreasing the level of liver enzymes, reducing the liver necrosis with vacuolization, decreasing the hepatic malondialdehyde formation, increasing hepatic antioxidants activities, suppressing the pro-inflammatory cytokines (Tumor Necrosis Factor, Interleukin-6 and Interleukin-1beta), inhibiting Nitric Oxide production, enhancing sulfotransferases and UDP-glucuronosyltransferases activities. Notably, the expression of cytochrome P450 2E1 was inhibited by Echinacoside in a dose-dependent manner and the binding energy was –214.3 MeV. Echinacoside showed a significant protective effect against Acetaminophen-induced hepatotoxicity through the inhibition of oxidative stress, the expression of pro-inflammatory cytokines and cytochrome P450 2E1 protein expression.

Keywords: Acetaminophen (APAP); Cytochrome P450 2E1 (CYP 2E1); Echinacoside (ECH); Hepatotoxicity

Highlights:
- ECH pretreatment showed the protective effect on APAP-induced liver injury in mice.
- ECH significantly elevated the intracellular antioxidant enzymes activities.
- ECH reduced the production of nitric oxide and hepatic lipid peroxidation in mice.
- ECH significantly inhibited the pro-inflammatory cytokines in hepatotoxic-mice.

Introduction

Despite the development of modern drug therapy, drug-induced liver injury (DILI) is the leading common cause of Acute Liver Failure (ALF) of which Acetaminophen (APAP) overdose or abuse is the common cause (about 50%) (Lin et al., 2018). Both oxidative stress and inflammatory responses are involved in APAP-induced liver injury (Wu et al., 2018). Many toxic chemicals and xenobiotics, including APAP, are metabolized by cytochrome P450 2E1 (CYP2E1) (Huang et al., 2016). APAP is rapidly absorbed in the intestine and metabolized in the liver. The majority (85–90%) of a therapeutic dose undergoes phase II conjugation to harmless sulfated and glucuronidase metabolites (de Achaval and Suarez-Almazor, 2011; McGill and Jaeschke, 2013). The remaining 10–15% APAP undergoes phase I oxidation by the hepatic cytochrome P-450 (CYP) pathway (mainly by CYP2E1) to NAPQI. NAPQI induced GSH depletion plays a critical role in APAP toxicity (Hinson et al., 1995), leading to the formation of reactive oxygen and

* **Corresponding authors:** Chen Chen and Xiaoying Zhang, Shaanxi University of Technology, College of Biological Science and Engineering, Chinese-German Joint Laboratory for Natural Product Research, Hanzhong, Shaanxi, China;
e-mail: cchen2008@yahoo.com; zhang@bio.uminho.pt; http://doi.org/10.32725/jab.2021.011

Submitted: 2020-01-21 • Accepted: 2021-04-19 • Prepublished online: 2021-04-26
J Appl Biomed 19/2: 105–112 • EISSN 1214-0287 • ISSN 1214-021X

nitrogen species, and initiates lipid peroxidation that eventually results in damage, necrosis or apoptosis of the liver cells (Rolando et al., 2000).

Echinacoside (ECH), a natural water-soluble phenylethanoid glycoside compound, was reported for its potentials in the prevention and treatment of various diseases and disorders by possessing strong antioxidant activities, exhibiting induction and/or activation of major endogenous antioxidant enzymes, inactivating pro-oxidant enzymes, neuroprotection, and anti-inflammatory activity (Liu et al., 2018; Shen et al., 2015). This study aims to investigate the effects of ECH against APAP-induced liver injury and to explore its potential mechanisms.

Materials and methods

Experimental animals

Five-week-old Kun-Ming male mice (28 ± 2 g) were purchased from the Experimental Animal Center of the Medical University of the Air Force (Xi'an, China). All mice were kept in an air- and humidity-controlled environment at 25 °C. The mice were adapted to the laboratory conditions for one week before the experiment and given access to standard food and distilled water (dH_2O) throughout the experiment. They were maintained at a laboratory temperature with constant humidity, as well as a 12 h light/12 h darkness cycle.

Animals and treatment

All experimental animal protocols were reviewed and approved by the institutional Committee of Shaanxi University of Technology for the use of laboratory animals (Number: 2019-009, Chinese–German Joint Laboratory for Natural Product Research), and the international guidelines for animal studies were followed (International Workshop..., 2004).

After 7 days of adaptation, a total of 42 male mice were randomly divided into the following 7 groups (n = 6): N/C (normal/control), APAP (300 mg/kg; model control group), ECH-only (100 mg/kg), low concentration ECH group ECHL (APAP + 25 mg/kg ECH), medium concentration ECH group ECHM (APAP + 50 mg/kg ECH), high concentration ECH group ECHH (APAP + 100 mg/kg ECH) and N-Acetyl Cysteine (NAC) group (APAP + 100 mg/kg NAC; positive control). The mice from the N/C groups were orally given distilled water. The ECH-only group was set up to test whether ECH is toxic to mice. The rest of the groups were treated with corresponding doses of NAC and the different concentrations of ECH intragastric administration for 7 days. All mice were intraperitoneally injected with APAP 1 h after the last treatment of NAC and the different concentrations of ECH on day 7. The control group and ECH-only group were injected with the same volume of normal saline. After treatment, mice were anesthetized with 1% sodium pentobarbital administered intraperitoneally (80 mg/kg). The blood and liver tissues were used for biological and histological evaluation. The mice blood was collected from eyes (retro-orbital) using heparinized tube, 24 h after the APAP challenge. The liver tissues were subsequently collected and washed with PBS for three times. Liver tissue samples were taken in 1.5 ml EP collection containers. The serum was separated from the blood samples by centrifugation at 1500× g for 10 min at 4 °C and stored at –80 °C until further analysis. The remaining liver tissues were thoroughly rinsed in cold 0.9% physiological saline and divided into small portions, then frozen in liquid nitrogen and stored at –80 °C for biochemical analysis.

DPPH radical scavenging

ECH-free radical scavenging capacity (RSC) was evaluated by measuring the 2, 2-diphenyl- 1-picrylhydrazyl- (DPPH) scavenging activity on 96-well microtiter plate (Boly et al., 2016). Different concentration of ECH (100 µl) were added to 100 µl of methanolic solution of DPPH (0.4 mM). The reaction mixture was incubated in darkness at room temperature for 30 min and absorbance was recorded at 517 nm. NAC was used for positive control; tests were carried out in triplicate. The radical scavenging activity was calculated as follows:

Scavenging % = [Absorbance of Control – Absorbance of Sample/Absorbance of Control] × 100%

Histological analysis

The liver lobe from each mouse was fixed in 10% formaldehyde phosphate buffer, embedded in paraffin, cut into sections (5 µm), and then stained with hematoxylin and eosin (H&E). Briefly, all steps for 60 min at room temperature. The histological examination was done under light microscopy (Olympus, Japan) at 400× magnification. The percentages of damaged cells were measured in the Trainable Weka Segmentation plugin in Fiji (version 3.2.20), an open-source machine learning and data mining toolkit based on the Waikato Environment for Knowledge Analysis (Weka, University of Waikato, Hamilton, New Zealand) (Sikpa et al., 2019). Briefly, three segmentation classes were created: background, normal and damaged cells. The specific area of damaged cells was calculated using thresholding techniques.

Determination of ALT and AST levels in serum

The blood samples were kept at room temperature for 2 h and then centrifuged at 1500× g for 10 min at 4 °C to obtain serum. The serum alanine aminotransferase (ALT) and aspartate aminotransferase (AST) levels were quantified using commercial kits, (Cat. No. C009-2-1 and C00-2-1 respectively, Nanjing Jiancheng Bioengineering Institute, Nanjing, China).

Determination of the SOD, CAT, GSH and MDA levels in liver tissues

The liver tissues were thawed and homogenized in the nine folds (g/ml) of ice-cold normal saline. The homogenate was centrifuged at 1500× g for 10 min at 4 °C to obtain the supernatant. The levels of superoxide dismutase (SOD), catalase (CAT), glutathione (GSH), and malondialdehyde (MDA) in the supernatant were measured using commercial kits, (Cat. No. A001-3-2, A007-1-1, A005-1-2 and A003-2, respectively, Jiancheng Bioengineering Institute, Nanjing, China). The protein concentrations in tissue homogenates were measured using a Bradford protein assay with bovine serum albumin as standard (Tiangen Biotech, Beijing, China).

Determination of Nitric Oxide production

The Nitric Oxide (NO) production of liver tissue supernatant was determined by Griess method (Saleh et al., 1999). Samples of liver tissue supernatant (50 µl) were added to each well in 96-well microplate in triplicate. Then, 50 µl of Griess reagent was added (1% sulfanilamide in 5% phosphoric acid and 0.1% N-(1-naphthyl) ethylenediamine dihydrochloride in Milli-Q water) at room temperature. After 10 min, the plate was read using ELISA plate reader at a wavelength of 550 nm. NO production was calculated from a standard curve of sodium nitrite.

Determination of TNF-α, IL-6 and IL-1β cytokines in serum

The levels of three inflammation-related factors, Tumor Necrosis Factor (TNF-α), Interleukin-6 (IL-6), and Interleukin-1beta

(IL-1β), were measured by commercial ELISA kits, (Cat. No. HO52, H007, and H002 respectively, Jiancheng Bioengineering Institute, Nanjing, China) according to the manufacturer's instructions. These experiments were performed in triplicate.

Measurement of SULTs and UGTs activities

Activities of sulfotransferases (SULTs) and UDP glucuronosyltransferases (UGTs) in liver microsome were determined using commercial ELISA kits (Cat. No. ML061414 and ML060442 respectively, Enzyme-linked Biotechnology, Shanghai, China).

Western blot analysis

For the microsomal preparation, the liver homogenate was centrifuged at 9000× g for 20 min at 4 °C, and the supernatant was transferred to a tube with 88 mM $CaCl_2$, after being shaken on ice for 5 min, the mixture was centrifuged at 27000× g for 20 min at 4 °C. The pellets were collected and resuspended in 50 mM Tris-HCl mixed with 20% glycerol. The protein concentration was determined using a BSA assay kit (Beyotime Institute of Biotechnology, Beijing, China).

Protein samples were extracted from liver tissue and separated by SDS-PAGE. After being transferred to PVDF membranes (Millipore Corporation, Boston, MA, USA), the membranes were blocked in TBST containing 5% skimmed milk powder and incubated overnight at 4 °C with primary antibodies (CYP2E1, 1 : 500, Cat. No. BA1774-2, Boster, Wuhan, China; β-actin 1 : 1000, Cat. No. LK9001T, Sungene Biotech, Tianjin, China). After washing three times with TBST, the membranes were incubated with horseradish peroxidase conjugated secondary antibodies (1 : 2000, Cat. No. LK2001, Sungene Biotech, Tianjin, China) for 2 h at room temperature. Protein bands were visualized by ECL reaction (Genshare Biological, Xi'an, China) and the protein levels were quantified using Gel-Pro Analyzer software (Media Cybernetics, Bethesda, USA) as normalized to beta-actin.

In silico *molecular docking*

Echinacoside (Ligand) and CYP2E1 (receptor) interaction was identified using Auto Dock Vina and iGEMDOCK v2.1 (Schrodinger, New York, USA). The ligand structure data was retrieved from PubChem (https://pubchem.ncbi.nlm.nih.gov/) and the target proteins were retrieved from the protein data bank (PDB, https://www.rcsb.org/) (Shen et al., 2010). The binding energy was evaluated by Lamarckian genetic algorithm method.

Statistical analysis

All experimental data were expressed as mean ± SD. The significant difference from the respective control in all experiments was assessed by one-way analysis of variance (ANOVA) using SPSS (IBM Corporation, Chicago, IL, USA) followed by Duncan Scheffe Bonferroni Sidak GT2 *post hoc* tests. Values of $p < 0.05$ were considered statistically significant. Statistical analysis was carried out using the Graph Pad Prism software v.7 (GraphPad Sofware, Inc, California, USA).

Results

ECH had strong free radical scavenging activity

The scavenging activity of ECH was evaluated spectrophotometrically by DPPH assay at doses from 3.125 to 100 μg/ml – which showed antioxidant activity at IC50 value of 10.05 μg/ml that was significantly lower than that of NAC 23.5 μg/ml (Fig. 1).

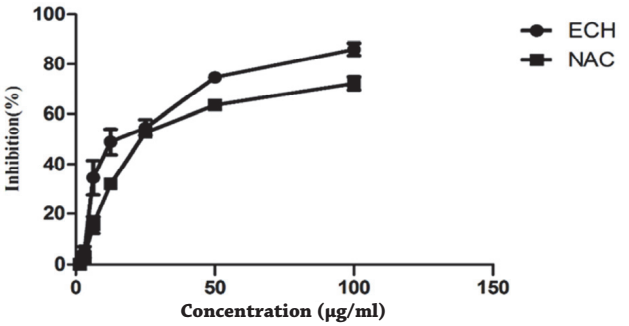

Fig. 1. Antioxidant activity of ECH on DPPH by DPPH-Assay compared with NAC (μg/ml)

ECH alleviated APAP-induced histopathological changes in liver

The liver histopathology showed characteristic histologic features in liver necrosis with vacuolization and inflammation in the APAP group. However, ECH pretreatments apparently alleviated such damage (Fig. 2). The ECHH group considerably changed the hepatic parenchyma similar to the morphology of the NC group. The hepatocytes in the ECHL and ECHM groups appeared normal, with limited cytoplasmic vacuolation observed in ECHL.

ECH attenuated APAP-induced liver enzyme dysfunction

The levels of ALT and AST were significantly increased in the APAP group compared to the NC group, confirming the hepatotoxicity of APAP (Fig. 3), while they were significantly reversed in the ECHH group ($p < 0.001$). ECHL and ECHM decreased the levels of ALT and AST, but without a convincing dose-effect relationship (Fig. 3).

ECH activated major liver antioxidant enzymes

The administration of APAP significantly ($p < 0.05$) decreased the activities of GSH, CAT and SOD compared with NC group while the decreased activities of major antioxidant enzymes were reversed by ECHH and NAC groups. ECHM and ECHL groups elevated the GSH, CAT and SOD levels (Fig. 4).

ECH inhibited APAP-induced lipid peroxidation

MDA levels were significantly ($p < 0.001$) increased in the APAP group. NAC significantly reversed this increase. And, ECH treatment suppressed the increase of MDA in a dosage--dependent manner (Fig. 5A).

ECH inhibited APAP-induced nitric oxide production

NO concentration in liver tissue was markedly increased in the APAP group, while ECHH significantly reversed the increase. Compared to N/C, ECH inhibited APAP-induced lipid peroxidation by suppressing MDA and NO increases in a dosage-dependent manner (Fig. 5B).

ECH inhibited the levels of major serum pro-inflammatory cytokines

The APAP overdose significantly increased the production of TNF-α, IL-6 and IL-1β (Fig. 6). However, these inflammatory cytokines were significantly decreased ($p < 0.001$) by the administration of ECH in different concentrations.

ECH activated the activities of SULTs and UGTs

SULTs and UGTs activities were significantly suppressed by APAP. ECH pre-administration reversed APAP-induced decrease in UGTs and SULTs in a dose-dependent manner (Fig. 7).

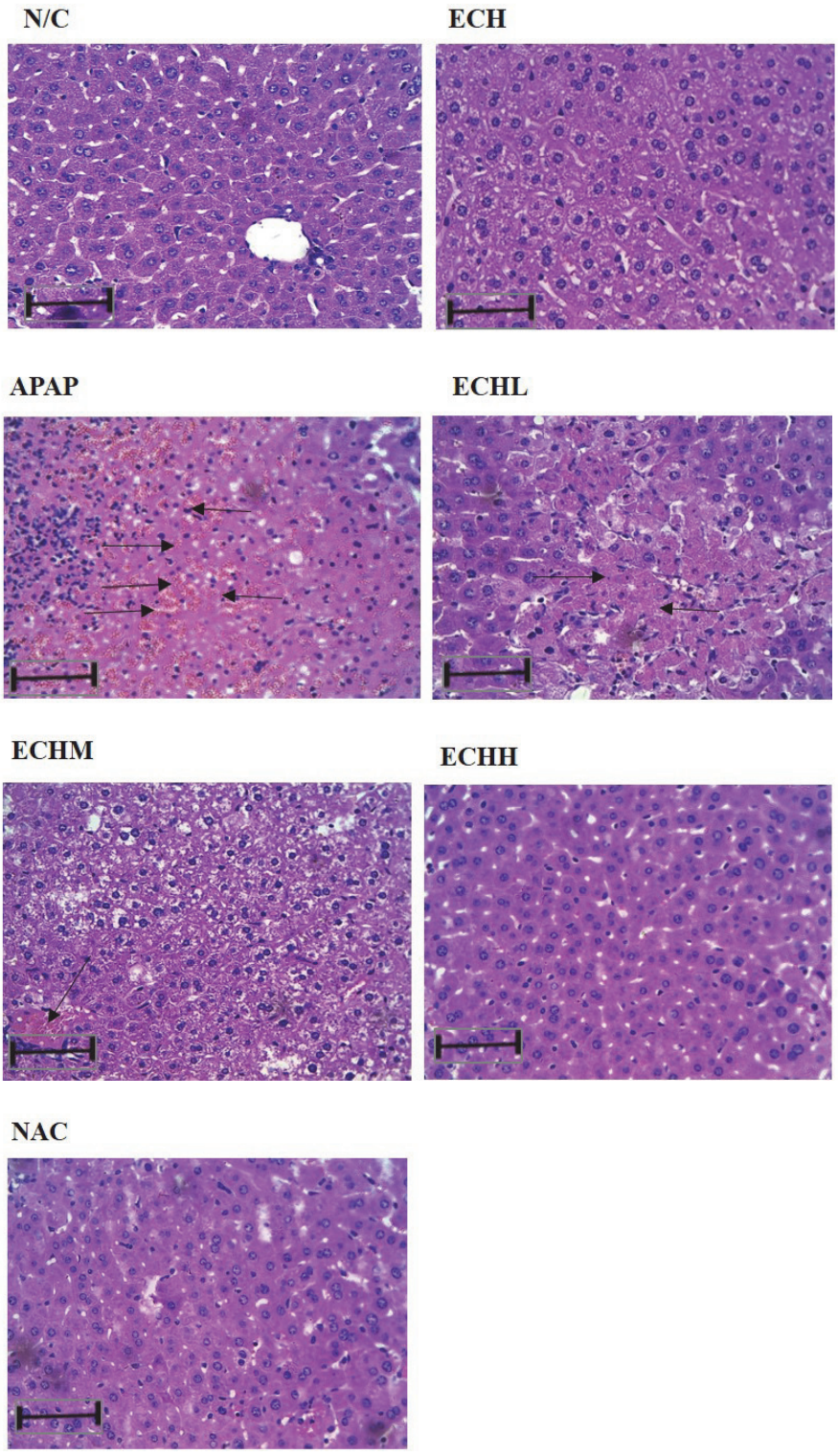

Fig. 2. Effects of ECH on hepatic histopathological alterations following Acetaminophen (APAP) treatment. **N/C** and **ECH** groups showed normal morphology, **APAP** and **ECHL** groups presented severe necrosis (black arrow marks indicate necrosis or extravasated blood), **ECHM**, **ECHH** and **NAC** groups were reversed similarly to N/C group. Hematoxylin and Eosin (H&E) staining of liver tissues. The original magnification is 400× and scale bar is 200 μm. The percentage of damaged cells in APAP group, ECHL group and ECHM group were 60.49%, 23.40% and 4.16% respectively.

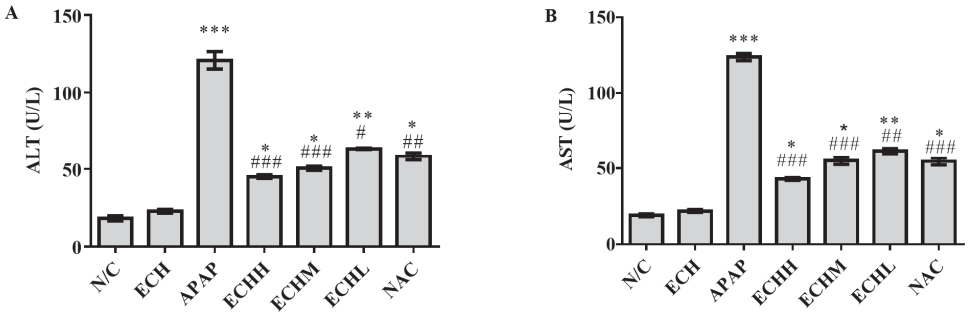

Fig. 3. Effects of ECH on APAP-induced (**A**) increased level of ALT and (**B**) increased level of AST. Data are expressed as mean M ± SD; $n = 6$; $^{*}p < 0.05$ and $^{***}p < 0.001$ compared with the control group; $\#p < 0.05$, $\#\#p < 0.01$ and $\#\#\#p < 0.001$ compared with the APAP group.

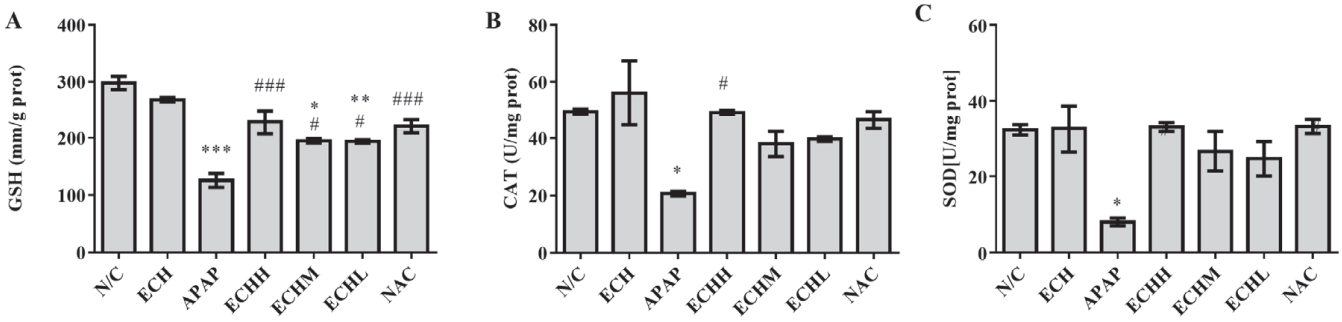

Fig. 4. Effects of ECH on the expression of antioxidant enzymes (**A**) GSH, (**B**) CAT and (**C**) SOD in liver tissues. Data are expressed as mean M ± SD; $n = 6$; $^{*}p < 0.05$ and $^{***}p < 0.001$ compared with the control group; $\#p < 0.05$, $\#\#p < 0.01$ and $\#\#\#p < 0.001$ compared with the APAP group.

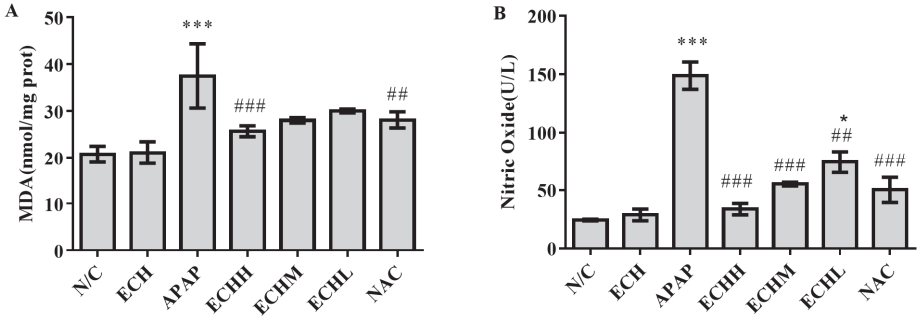

Fig. 5. Effects of ECH on (**A**) lipid peroxide level and (**B**) nitric oxide level. Data are expressed as mean M ± SD; $n = 6$; $^{*}p < 0.05$ and $^{***}p < 0.001$ compared with the control group; $\#p < 0.05$, $\#\#p < 0.01$ and $\#\#\#p < 0.001$ compared with the APAP group.

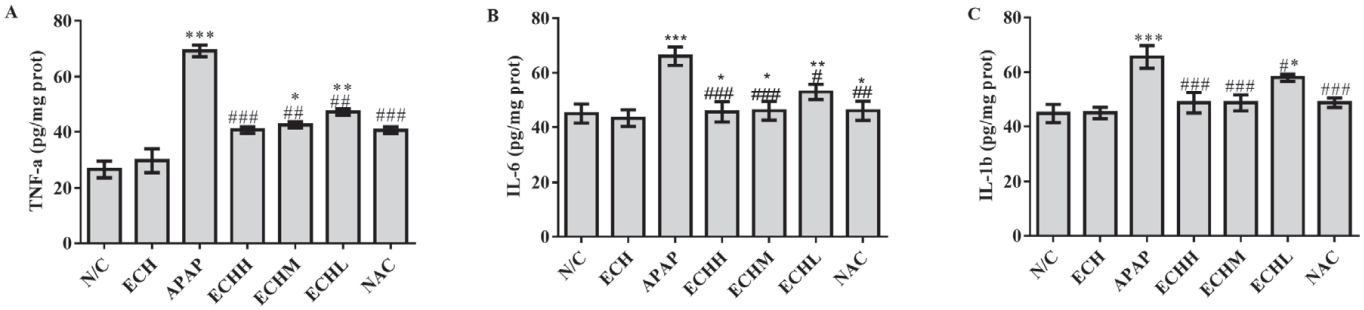

Fig. 6. Effects of ECH on serum (**A**) TNF-α, (**B**) IL-6 and (**C**) IL-1β. Data are expressed as mean M ± SD; $n = 6$; $^{*}p < 0.05$ and $^{***}p < 0.001$ compared with the control group; $\#p < 0.05$, $\#\#p < 0.01$ and $\#\#\#p < 0.001$ compared with the APAP group.

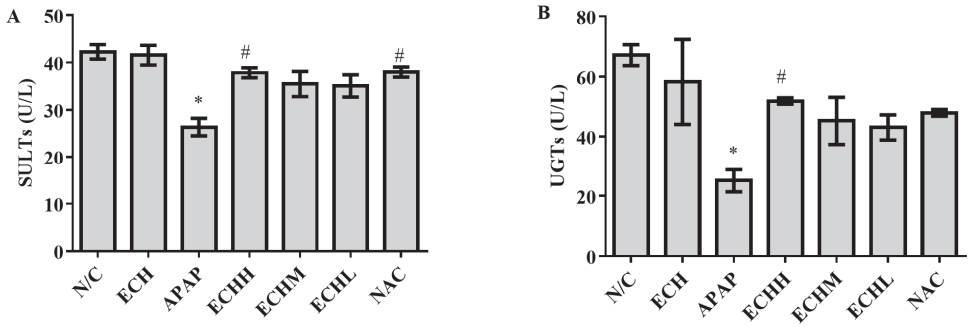

Fig. 7. Effects of ECH on the activities of (**A**) SULTs and (**B**) UGTs determined by ELISA. Data are expressed as mean M ± SD; $n = 6$; $^{*}p < 0.05$ and $^{***}p < 0.001$ compared with the control group; $\#p < 0.05$, $\#\#p < 0.01$ and $\#\#\#p < 0.001$ compared with the APAP group.

ECH suppressed CYP2E1 expression on APAP-induced liver injury

The expression levels of cytochrome P450 2E1 (CYP2E1) protein were obviously increased in the APAP group. However, the pretreatments of ECH in different concentrations, as well as NAC, suppressed the CYP2E1 protein expression (Fig. 8).

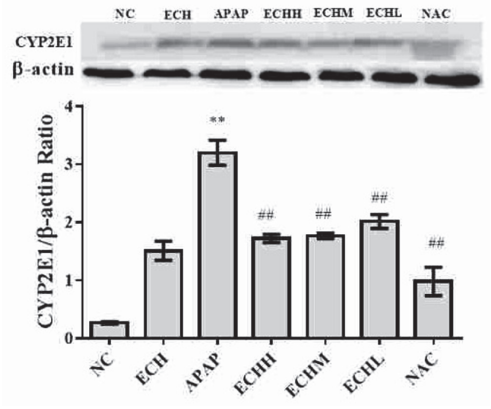

Fig. 8. Effect of ECH on APAP-induced inhibitory CYP2E1 expression in liver tissue. Data are expressed as mean M ± SD; $n = 6$; $^{*}p < 0.05$ and $^{***}p < 0.001$ compared with the control group; $\#p < 0.05$, $\#\#p < 0.01$ and $\#\#\#p < 0.001$ compared with the APAP group.

ECH binds to CYP2E1 in docking

The molecular docking study further elucidated the binding sites of the ECH and CYP2E1.

The binding energy between ECH and CYP2E1 was –214.3 and the hydrogen interaction sites were Thr (Threonine) 304, Leu (Leucine) 364, Cys (Cysteine) 437 and Lzi (A leucine zipper) 501 (Fig. 9).

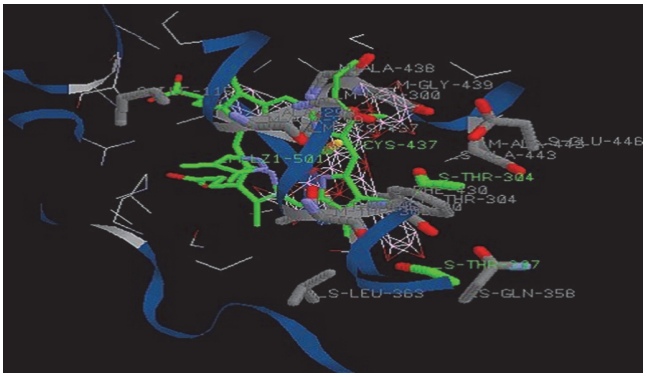

Fig. 9. Interaction sites of ECH with CYP2E1. Green represented the interaction sites of Thr 304, Leu 364, Cys 437 and Lzi 501 on CYP2E1, blue represented hydrogen interaction, red represented Ligand.

Discussion

ECH, a natural phenylethanoid glycoside, is a major phenolic component in *Echinacea angustifolia* and *E. pallida* roots which are an important traditional Chinese medicine used for the treatment of kidney deficiency and neurodegenerative diseases (Jia et al., 2006). ECH was also separated and purified from an ethanol extract of *Cistanche tubulosa* (Schenk) R. which are widely used in Europe, North America and Australia for their immunostimulating activities (Jia et al., 2008). ECH (111670-200503, National Institutes for Food and Drug Control, China) was used as standard compound of Phenylethanoid glycosides (PhGs), and these PhGs compounds are the major active constituents of *Cistanche tubulosa* (Wang et al., 2016). Recently, ECH, as a promising candidate compound, has been proved to have a broad pharmacological effect, including neuroprotective, immunomodulatory, hormonal balancing, anti-fatigue, anti-inflammatory, hepatoprotection, anti-oxidative, anti-bacterial, anti-viral, and anti-tumor effects, etc. (Fu et al., 2018). We investigated the effects of ECH on the sperm quality and hormone levels on a male mice model, demonstrating that ECH has the drug ability as a tonic agent to cure reproductive dysfunction (Jiang et al., 2016; Jiang et al., 2018), the herbs enriched in ECH, such as *Cistanche tubulosa*, have been included in different pharmacopeia.

It is necessary to address that different independent research groups have confirmed hepatoprotective effects of ECH in lipopolysaccharide (LPS)-induced acute liver injury (ECH 60 mg/kg) (Li et al., 2014) in mice. Several studies have shown that *Cistanche tubulosa* and ECH have hepatoprotective properties against chronic alcohol-induced liver injury in mice (Guo et al., 2016; Luo et al., 2016; You et al., 2015).

In our present study, compared to the N/C group, the levels of ALT and AST in the APAP group were 6.7 and 6.5 times higher. However, they are lower compared to some other studies at

this dose and time point (Papackova et al., 2018; Xiong et al., 2017). This may be attributed to the difference of mice breed. However, essential biomarkers (ALT and AST) were elevated by APAP overdose hepatotoxicity (Fig. 3). These major biomarkers indicate a relatively severe liver injury, leading to hepatic dysfunction and mitochondrial damage due to oxidation or inflammation (Uchida et al., 2017). And ECH treatment significantly attenuated APAP overdose and induced the increase of serum ALT, AST and hepatic histopathological lesions.

Our results demonstrated that in the histopathological examination, hepatic morphology showed an extensive hepatocyte necrosis area with extravasated blood and vacuolization in APAP treated mice. But it was clearly shown that vacuolization and necrosis in APAP-induced mice were attenuated by the pretreatment of ECH groups and NAC group. These results suggest that ECH possesses the ability to prevent APAP-induced hepatotoxicity.

APAP-induced hepatotoxicity increases ROS level and leads to oxidative stress that, as a result, decreases cellular GSH level and reduces the activity of antioxidant enzymes such as SOD and CAT. Lipid peroxidation reflexes the oxidative process in the body. MDA, as a sensitive biomarker of oxidative stress, is one of the products of lipid peroxidation (Cigremis et al., 2009; Nikravesh et al., 2018; Slattery et al., 2014). In the present study, APAP administration significantly reduced liver antioxidant capacity, and we found that administration of ECH significantly increased the lessening of SOD, CAT and GSH, and suppressed the increase of MDA caused by APAP in liver tissues. In this study, ECH could effectively reduce hepatic lipid peroxidation level in a dose-dependent manner by inhibiting the formation of MDA. These results of our study indicated that the ECH scavenged ROS through the up regulation of intracellular antioxidant enzyme activity and highly increased the resistance to APAP-induced oxidative burden. NO, a pro-inflammatory mediator and highly reactive oxidant free radical is overproduced under inflammatory conditions, and may react with various ROS form peroxynitrite, cause cytotoxic and provoke lipid peroxidation (Beckman et al., 1990). This study investigated that the NO production conversely changed in liver tissue in ECH groups, indicating a protective effect of ECH in reducing lipid peroxidation and peroxynitrite radical due to the effect of anti-oxidant and anti-inflammatory activities.

Inflammatory mediators, pro-inflammatory cytokines, such as IL-1β, IL-6 and TNF-α are precursors of APAP-induced liver injury (Li et al., 2018). Therefore, down-regulating the effect of these pro-inflammatory cytokines was considered an effective strategy for APAP-induced hepatic damage. In the present study, we found that ECH reversed the increased pro-inflammatory cytokines IL-1β, IL-6 and TNF-α in liver tissue, demonstrating that ECH possesses anti-inflammatory activity and subsequently decreases the secretion of the pro-inflammatory cytokines in APAP-treated mice.

Elimination of APAP takes place in the liver, where the majority of APAP is either glucuronidated or sulfate and then excreted in the urine. UGT1A6 and UGT1A1 are major enzymes involved in APAP glucuronidation, making a high contribution to APAP clearance. SULTs are responsible for the formation of APAP sulfation in both rats and humans (Nakagawa et al., 2012). The increase of hepatic UGTs and SULTs enhanced the resistance to APAP toxicity in mice and plays an important role in the detoxification of APAP (Fakurazi et al., 2012; Fan et al., 2013). In the present study, ECH markedly enhanced the activities of UGTs and SULTs (Fig. 7), indicating ECH was able to accelerate the biotransformation of APAP glucuronidation and sulfation.

High level of CYP2E1 expression in liver involved the production of free radicals in the APAP-induced hepatotoxicity, thus leading to decreased hepatic GSH, increased lipid peroxidation and inflammation (Papackova et al., 2018). According to the western blot analysis, CYP2E1 protein expression was enhanced by APAP. However, CYP2E1 level was markedly suppressed by the ECHM group. ECH in different concentrations decreased CYP2E1 expression compared with the APAP group. Indeed, ECH-only treatment (100 mg/kg, high concentration) increased the CYP2E1 ratio as compared to the NC group. In our study, ECH-H did not show an obvious better effect on mice as compared to ECH-M. Further investigation on the safety assessment and optimal dosing of ECH are needed.

Conclusions

ECH has a hepatoprotective effect through the reduction of CYP2E1 activities, elevation of intracellular antioxidant enzymes activities, decrease of the lipid peroxidation and NO production, and suppressing the pro-inflammatory cytokines as well as up-regulation on the expression and activities of detoxification enzymes including UGTs and SULTs.

Conflict of interests

The authors declare that there is no conflict of interests.

Author contribution

Dr. XYZ designed the study; Dr. MT and BL performed the study; Dr. MT analyzed data, and prepared the manuscript; XYZ collected the data of the study; CC analyzed the data. All authors have read and approved the manuscript.

Acknowledgements

Thanks to the other lab members of Shaanxi University of Technology for their help.

Ethical approval and consent to participate

All experimental animal protocols were reviewed and approved by the institutional Committee of Shaanxi University of Technology for the use of laboratory animals (Number: 2019-009, Chinese-German Joint Laboratory for Natural Product Research), and the international guidelines for animal studies were followed.

Funding

This work was supported by grants from the national Key Research and Development Program of China [grant number 2017YFD0501405]; Innovation Capability Support Program of Shaanxi [grant number 2019XY-04]; Talented Young Scientist Program (TYSP) sponsored by China Science and Technology Exchange Center (CSTEC), and International Youth Education Project Special Funds.

References

Beckman JS, Beckman TW, Chen J, Marshall PA, Freeman BA (1990). Apparent hydroxyl radical production by peroxynitrite: implications for endothelial injury from nitric oxide and superoxide. Proc Natl Acad Sci U S A 87(4): 1620–1624. DOI: 10.1073/pnas.87.4.1620.

Boly R, Lamkami T, Lompo M, Dubois J, Guissou IP (2016). DPPH Free Radical Scavenging Activity of Two Extracts from *Agelanthus dodoneifolius* (Loranthaceae) Leaves. Int J Toxicol Pharmacol Res 8(1): 29–34.

Cigremis Y, Turel H, Adiguzel K, Akgoz M, Kart A, Karaman M, Ozen H (2009). The effects of acute acetaminophen toxicity on hepatic mRNA expression of SOD, CAT, GSH-Px, and levels of peroxynitrite, nitric oxide, reduced glutathione, and malondialdehyde in rabbit. Mol Cell Biochem 327(1–2): 277. DOI: 10.1007/s11010-009-0093-6.

de Achaval S, Suarez-Almazor M (2011). Acetaminophen overdose: a little recognized public health threat. Pharmacoepidemiol Drug Saf 20(8): 827–829. DOI: 10.1002/pds.2162.

Fakurazi S, Sharifudin SA, Arulselvan P (2012). *Moringa oleifera* hydroethanolic extracts effectively alleviate acetaminophen-induced hepatotoxicity in experimental rats through their antioxidant nature. Molecules 17(7): 8334–8350. DOI: 10.3390/molecules17078334.

Fan Y-J., Rong Y, Li P-F, Dong W-L, Zhang D-Y, Zhang L, Cui M-J (2013). Genistein protection against acetaminophen-induced liver injury via its potential impact on the activation of UDP-glucuronosyltransferase and antioxidant enzymes. Food Chem Toxicol 55: 172–181. DOI: 10.1016/j.fct.2013.01.003.

Fu Z, Fan X, Wang X, Gao X (2018). Cistanches Herba: An overview of its chemistry, pharmacology, and pharmacokinetics property. J Ethnopharmacol 219: 233–247. DOI: 10.1016/j.jep.2017.10.015.

Guo Y, Cao L, Zhao Q, Zhang L, Chen J, Liu B, Zhao B (2016). Preliminary characterizations, antioxidant and hepatoprotective activity of polysaccharide from *Cistanche deserticola*. Int J Biol Macromol 93(Pt A): 678–685. DOI: 10.1016/j.ijbiomac.2016.09.039.

Hinson JA, Pumford NR, Roberts DW (1995). Mechanisms of acetaminophen toxicity: immunochemical detection of drug-protein adducts. Drug Metab Rev 27(1–2): 73–92. DOI: 10.3109/03602539509029816.

Huang Y-J, Chen P, Lee C-Y, Yang S-Y, Lin M-T, Lee H-S, Wu Y-M (2016). Protection against acetaminophen-induced acute liver failure by omentum adipose tissue derived stem cells through the mediation of Nrf2 and cytochrome P450 expression. J Biomed Sci 23: 5. DOI: 10.1186/s12929-016-0231-x.

International Workshop on Development of Science-Based Guidelines for Laboratory Animal Care (2004). Proceedings of the November 2003 International Workshop.

Jia C, Shi H, Jin W, Zhang K, Jiang Y, Zhao M, Tu P (2008). Metabolism of Echinacoside, a Good Antioxidant, in Rats: Isolation and Identification of Its Biliary Metabolites. Drug Metab Dispos 37(2): 431–438. DOI: 10.1124/dmd.108.023697.

Jia C, Shi H, Wu X, Li Y, Chen J, Tu P (2006). Determination of echinacoside in rat serum by reversed-phase high-performance liquid chromatography with ultraviolet detection and its application to pharmacokinetics and bioavailability. J Chromatogr B Analyt Technol Biomed Life Sci 844(2): 308–313. DOI: 10.1016/j.jchromb.2006.07.040.

Jiang Z, Wang J, Li X, Zhang X (2016). Echinacoside and *Cistanche tubulosa* (Schenk) R. wight ameliorate bisphenol A-induced testicular and sperm damage in rats through gonad axis regulated steroidogenic enzymes. J Ethnopharmacol 193: 321–328. DOI: 10.1016/j.jep.2016.07.033.

Jiang Z, Zhou B, Li X, Kirby GM, Zhang X (2018). Echinacoside Increases Sperm Quantity in Rats by Targeting the Hypothalamic Androgen Receptor. Scientific Reports 8(1). DOI: 10.1038/s41598-018-22211-1.

Li L, Huang W, Wang S, Sun K, Zhang W, Ding Y, et al. (2018). Astragaloside IV Attenuates Acetaminophen-Induced Liver Injuries in Mice by Activating the Nrf2 Signaling Pathway. Molecules 23(8): 2032. DOI: 10.3390/molecules23082032.

Li X, Gou C, Yang H, Qiu J, Gu T, Wen T (2014). Echinacoside ameliorates D-galactosamine plus lipopolysaccharide-induced acute liver injury in mice via inhibition of apoptosis and inflammation. Scand J Gastroenterol 49(8): 993–1000. DOI: 10.3109/00365521.2014.913190.

Lin G, Luo D, Liu J, Wu X, Chen J, Huang Q, et al. (2018). Hepatoprotective Effect of Polysaccharides Isolated from *Dendrobium officinale* against Acetaminophen-Induced Liver Injury in Mice via Regulation of the Nrf2-Keap1 Signaling Pathway. Oxid Med Cell Longev 2018: 6962439. DOI: 10.1155/2018/6962439.

Liu J, Yang L, Dong Y, Zhang B, Ma X (2018). Echinacoside, an Inestimable Natural Product in Treatment of Neurological and other Disorders. Molecules 23(5): 1213. DOI: 10.3390/molecules23051213.

Luo H, Cao R, Wang L, Zhu L (2016). Protective effect of Cistanchis A on ethanol-induced damage in primary cultured mouse hepatocytes. Biomed Pharmacother 83: 1071–1079. DOI: 10.1016/j.biopha.2016.08.028.

McGill MR, Jaeschke H (2013). Metabolism and disposition of acetaminophen: recent advances in relation to hepatotoxicity and diagnosis. Pharm Res 30(9): 2174–2187. DOI: 10.1007/s11095-013-1007-6.

Nakagawa T, Mure T, Yusoff S, Ono E, Harahap ISK, Morikawa S, et al. (2012). Acetaminophen administration in a patient with Gilbert's syndrome. Pediatr Int 54(6): 934–936. DOI: 10.1111/j.1442-200X.2012.03602.x.

Nikravesh H, Khodayar MJ, Mahdavinia M, Mansouri E, Zeidooni L, Dehbashi F (2018). Protective Effect of Gemfibrozil on Hepatotoxicity Induced by Acetaminophen in Mice: the Importance of Oxidative Stress Suppression. Adv Pharm Bull 8(2): 331–339. DOI: 10.15171/apb.2018.038.

Papackova Z, Heczkova M, Dankova H, Sticova E, Lodererova A, Bartonova L, et al. (2018). Silymarin prevents acetaminophen-induced hepatotoxicity in mice. PLoS One 13(1): e0191353. DOI: 10.1371/journal.pone.0191353.

Rolando N, Wade J, Davalos M, Wendon J, Philpott-Howard J, Williams R (2000). The systemic inflammatory response syndrome in acute liver failure. Hepatology 32(4 Pt 1): 734–739. DOI: 10.1053/jhep.2000.17687.

Saleh TS, Calixto JB, Medeiros YS (1999). Effects of anti-inflammatory drugs upon nitrate and myeloperoxidase levels in the mouse pleurisy induced by carrageenan. Peptides 20(8): 949–956. DOI: 10.1016/S0196-9781(99)00086-8.

Shen J, Tan C, Zhang Y, Li X, Li W, Huang J, Shen X, Tang Y (2010). Discovery of potent ligands for estrogen receptor beta by structure-based virtual screening. J Med Chem 53(14): 5361–5365. DOI: 10.1021/jm100369g.

Shen J-Y, Yang X-L, Yang Z-L, Kou J-P, Li F (2015). Enhancement of absorption and bioavailability of echinacoside by verapamil or clove oil. Drug Des Devel Ther 9: 4685–4693. DOI: 10.2147/DDDT.S87581.

Sikpa D, Fouquet JP, Lebel R, Diamandis P, Richer M, Lepage M (2019). Automated detection and quantification of breast cancer brain metastases in an animal model using democratized machine learning tools. Sci Rep 9(1): 17333. DOI: 10.1038/s41598-019-53911-x.

Slattery K, Bentley D, Coutts AJ (2014). The role of oxidative, inflammatory and neuroendocrinological systems during exercise stress in athletes: implications of antioxidant supplementation on physiological adaptation during intensified physical training. Sports Med 45(4): 453–471. DOI: 10.1007/s40279-014-0282-7.

Uchida NS, Silva-Filho SE, Cardia GFE, Cremer E, de Souza Silva-Comar FM, Silva EL, et al. (2017). Hepatoprotective Effect of Citral on Acetaminophen-Induced Liver Toxicity in Mice. Evid Based Complement Alternat Med 2017: 1796209. DOI: 10.1155/2017/1796209.

Wang T, Chen C, Yang M, Deng B, Kirby GM, Zhang X (2016). *Cistanche tubulosa* ethanol extract mediates rat sex hormone levels by induction of testicular steroidgenic enzymes. Pharm Biol 54(3): 481–487. DOI: 10.3109/13880209.2015.1050114.

Wu K-C, Ho Y-L, Kuo Y-H, Huang S-S, Huang G-J, Chang Y-S (2018). Hepatoprotective Effect of Ugonin M, A *Helminthostachys zeylanica* Constituent, on Acetaminophen-Induced Acute Liver Injury in Mice. Molecules 23(10): 2420. DOI: 10.3390/molecules23102420.

Xiong X, Ren Y, Cui Y, Li R, Wang C, Zhang Y (2017). Obeticholic acid protects mice against lipopolysaccharide-induced liver injury and inflammation. Biomed Pharmacother 96: 1292–1298. DOI: 10.1016/j.biopha.2017.11.083.

You S-P, Zhao J, Ma L, Tudimat M, Zhang S-L, Liu T (2015). Preventive effects of phenylethanol glycosides from *Cistanche tubulosa* on bovine serum albumin-induced hepatic fibrosis in rats. Daru 23: 52. DOI: 10.1186/s40199-015-0135-4.